

Detection and Classification of Mosaic Virus Disease in Cassava Plants by Proximal Sensing of Photochemical Reflectance Index

Sadasivan Nair Raji¹ · Narayanan Subhash^{1,3} · Velumani Ravi² · Raju Saravanan² ·
Changatharayil N. Mohanan¹ · Thangaraj MakeshKumar² · Sukumar Nita¹

Received: 13 November 2015 / Accepted: 3 February 2016 / Published online: 12 March 2016
© Indian Society of Remote Sensing 2016

Abstract Cassava Mosaic virus Disease (CMD) is the most severe and widespread virus infection that affects cassava (*Manihot esculenta* Crantz) crops. This paper investigates the application of photochemical reflectance index (PRI) imaging to detect and assess the impact of varying levels of CMD infection in cassava. Towards this, narrow band reflectance images of field-grown cassava plants were recorded at 531 and 571 nm by proximal sensing with a multispectral imaging system (MSIS). It was observed that the PRI values increase with increasing levels of CMD infection in all the varieties of cassava studied. A scatter plot of the PRI image intensity yielded a sensitivity of 85 % and specificity of 79 % for discriminating visibly no CMD from initial CMD and a sensitivity of 93 % and specificity of 92 % for discriminating initial CMD from advanced CMD. Area under the receiver operator characteristics (AUC-ROC) curve was used to discriminate the CMD infection level by differentiating visibly no CMD from initial CMD [AUC = 0.92] and initial CMD from advanced CMD [AUC = 0.99]. It was observed that PRI values determined from the experimental data follow a linear inverse relationship with net photosynthetic rate (P_n) ($R^2 = 0.76$) and total leaf chlorophyll (Chl) content ($R^2 = 0.80$). The results show that PRI imaging can be utilized

to discriminate healthy plants from CMD and other stress infected crops by proximal sensing in outdoor plants.

Keywords Photochemical reflectance index · Proximal sensing · Cassava mosaic disease · Virus infection · AUC-ROC

Introduction

Cassava (*Manihot esculenta* Crantz) popularly known as tapioca is an important staple food and industrial crop to a large population in Asia, Africa and Latin America. Among the various infections reported, cassava mosaic virus disease (CMD) is the most prevalent, which causes considerable crop damage and yield reduction, (Thresh et al. 1994; Patil and Fauquet 2009). CMD which is considered as a major constraint for cassava cultivation is transmitted by white flies or by vegetative propagation. Typical symptoms of CMD consist of a yellow or pale green chlorotic mosaic of leaves, commonly accompanied by distortion and crumbling. CMD affected leaves appear reduced in size, twisted and distorted. Some of the current diagnostic techniques, such as ELISA (Enzyme Linked Immuno Sorbent Assay), DIBO (Dot Immono Blot Assay) and PCR (Polymerase Chain Reaction) are costly and time consuming. These techniques follow destructive sampling followed by biochemical and molecular determination which involves molecular level processing of elaborate data and is labor and time consuming. Moreover, the reagents used for the detection are to be carefully selected as they are specific to each pathogen. In this context, novel techniques like fluorescence and reflectance imaging are found to be effective tools in the monitoring of vegetation and its stress. Various fluorescence and reflectance indices have been used by the scientific community in the detection of different types of stresses.

✉ Narayanan Subhash
subhashnarayanan@gmail.com

¹ National Center for Earth Science Studies, Akkulam, Thiruvananthapuram, Kerala 695031, India

² Central Tuber Crops Research Institute, Sreekariyam, Thiruvananthapuram, Kerala 695017, India

³ Forus Health Pvt Ltd., 23rd Cross, BSK-II, Banashankari, Bangalore, Karnataka 5600070, India

Photochemical Reflectance Index (PRI) is a physiological index that is related to the xanthophyll cycle and pigment content (Gamon et al. 1992), and provides information on the leaf physiological properties (Penuelas et al. 1994). During photosynthesis, when the absorbed light energy exceeds the photosynthetic capacity of the plant, the excess energy is dissipated by various mechanisms to avoid damage to the photosynthetic apparatus. The xanthophyll cycle is one such mechanism, wherein with increase in the incident light the xanthophyll pigments in the leaf gets converted from the epoxidized (violaxanthin) state to the de-epoxidized (antheraxanthin and zeaxanthin) state to dissipate the excess energy (Demmig-Adams and Adams 1994). This reaction is readily reversed under limiting light (Gamon et al. 1992). Filella et al. (2009) has reported that the de-epoxidation state can be used as an indicator of the short-term changes in photosynthetic activity.

Several studies have focused on the assessment of PRI at the leaf and the canopy level across ecosystems to track changes in photosynthesis with various factors like elevation and latitude (Richardson and Berlyn 2002; Richardson et al. 2003), plant diseases, soil water content and nutrient level variability (Whitehead et al. 2005; Panigada et al. 2014). This is due to the fact that the spectral indicator, PRI at 531 nm and 571 nm correlates with the xanthophylls cycle (Nichol and Grace 2010), and it determines the photosynthetic performance of plants (Bilger and Bjorkman 1990; Penuelas et al. 1997). Changes in leaf pigments of the xanthophyll cycle lead to changes in the reflectance at 531 nm whereas, the reflectance at 571 nm is insensitive to short term changes in leaf pigments and hence, the reflectance at 571 nm is used as a reference to reduce the effects of chloroplast movements. Penuelas et al. (1994, 1997) has reported that reflectance at 571 nm can also be used to normalize the reflectance at 531 nm and correct for non-uniformity of solar reflectance. Results of all these studies point to the fact that PRI has the potential to be used as a non-destructive technique to assess photosynthetic and other physiological changes associated with biotic and abiotic stresses in plants.

Imaging techniques has emerged as a fast and reliable method in plant disease detection, which can be used for continuous proximal and remote monitoring of physiological health status of plants (Carter and Miller 1994). The major advantage of proximal or remote sensing imaging is that it provides spatial information about the plant damage and covers large areas of vegetation in a short duration of time using passive sunlight as the source of light (Deery et al. 2014). The use of sunlight adds to the advantage that no additional light source is required to induce reflectance, but restricts its application to clear sky conditions. PRI imaging was carried out during noon time when there is minimal path length for solar radiation to reach earth's surface and the effects of ground reflection and shadows are minimal (Carter and Miller 1994).

Recently, Raji et al. (2015) has shown sunlight-induced fluorescence imaging to be an effective tool in the detection of mosaic virus disease in cassava plants. The present study explores the possibility of using PRI in the detection and classification of different levels of cassava mosaic virus (CMD) infection in potted plants by proximal imaging. This study was conducted to confirm that this technique could be used to mark the difference in degree of infection. This information could be used in the case when the plants are used as production materials, or extrapolating this research to other valuable crop species. Towards this, reflectance images of different varieties of potted cassava plants with varying degrees of CMD infection were recorded with a multi-spectral imaging system (MSIS). The photosynthetic rate (Pn) and chlorophyll (Chl) content of the plant leaves were correlated with the PRI image data and scatter plots were drawn to classify different levels of CMD infection, and the results are presented.

Materials and Methods

Plant Growth and Experimental Design

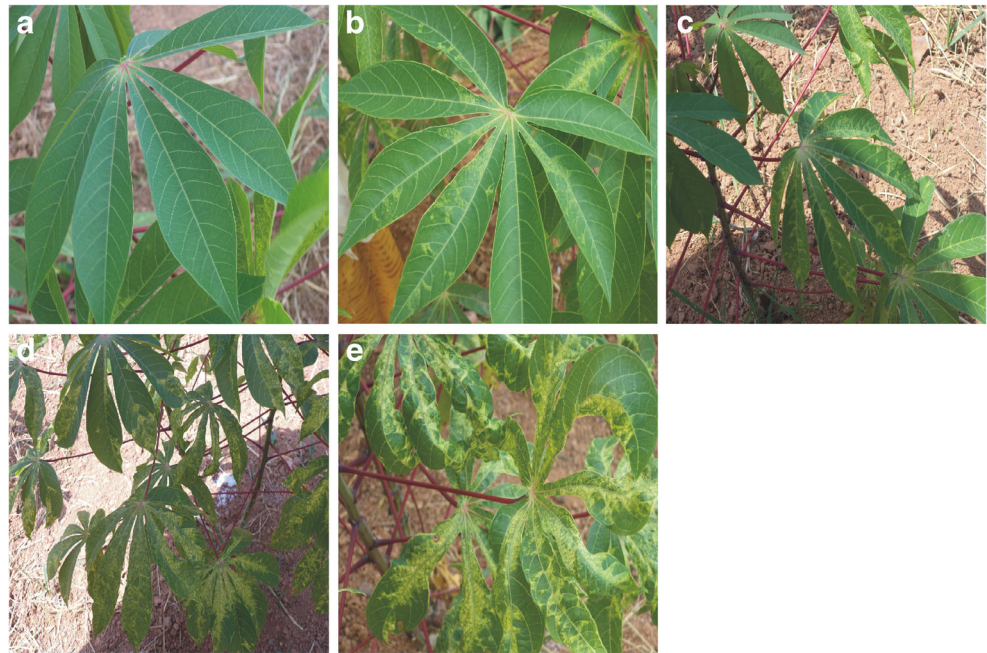
Stem cuttings of 14 varieties of cassava, each 20 cm long, were grown in pots filled with mixture of soil, farm yard mixture and sand at a ratio of 2:1:1 respectively. Rock phosphate was also added to the potting mixture as basal at the time of planting. Urea and muriate of potash were added after one week of planting and one month later. Three replicates were maintained for each variety of cassava and the plants were irrigated daily. Stem cuttings of cassava plants tested with varying levels of CMD were used as mother plants to grow infected plants.

The cassava plant leaves under study was categorized according to the level of mosaic infection from Grade 1–4 following the system developed by Terry (1975) (Table 1) and plant leaves without any visible symptom of infection were considered as normal (Fig. 1). The study was carried out in 14

Table 1 Categorization of cassava mosaic virus disease in infected leaves

CMD Grade	Symptoms
Normal/no CMD visible	Leaves with no visible symptoms of mosaic or no reduction in leaf area
Grade 1	Mosaic specks only, which may get masked
Grade 2	Only mild mosaic distributed on leaflets. No reduction in leaf area
Grade 3	Severe mosaic with 1/3 leaf area reduction usually at the base of leaflets
Grade 4	Severe mosaic with less than 2/3 leaf area reduction

Fig. 1 Cassava plants showing symptoms of cassava mosaic virus disease (CMD), leaf distortion and chlorosis. **a** normal/visibly no CMD **b** grade-1 CMD **c** grade-2 CMD **d** grade-3 CMD **e** grade-4 CMD



varieties of cassava viz., variety 1) Mulluvadi, variety 2) M-4, variety 3) 4–2, variety 4) M833, variety 5) H165, variety 6) H226, variety 7) Sree Jaya, variety 8) Sree Vijaya, variety 9) Sree Prakash, variety 10) Kumkum Rose, variety 11) 1687, variety 12) Thailand, variety 13) CI848 and variety 14) Quintal. Data collection was initiated after the plants were 8-weeks old.

Multi-Spectral Imaging System

Multi Spectral Imaging System (MSIS) developed for sunlight-induced fluorescence imaging of outdoor plants (Raji et al. 2015) was modified with filters at 531 and 571 nm, suitable for PRI estimation. This system (Fig. 2) consists of an Electron Multiplying CCD monochrome (EMCCD) camera with 1024 × 1024 pixels (Model: LUCA-R-DL-604, Andor Technology, UK), a Nikon AF 35-70 mm (1:1.8) zoom lens and narrow band (1 nm, FWHM) interference filters on the rotating filter mount. The camera is connected to the USB port of a laptop computer for control and data acquisition. Image processing was carried out using proprietary Andor SOLIS (Solutions for Imaging and Spectroscopy) software, which is a generic camera control and analysis software. Images were recorded from potted cassava plants on each day between 11.30 and 13.30 h for 7 days under clear sky conditions in March 2013 and full sunlight. During this time of the day, when the sun is at the zenith, the transmission path for solar irradiance and the effect of ground reflection would be minimal (Carter and Miller 1994). A reflectance standard (SRS-99-010- Labsphere, USA) was used as reference to normalize the captured images and to correct for any spatial

sensitivity characteristics within the viewed images (Nakaji et al. 2006). The resulting reflectance image R for each wavelength λ was calculated as follows:

$$R_{\lambda} = [I_{\lambda}/r_{\lambda}]K \tag{1}$$

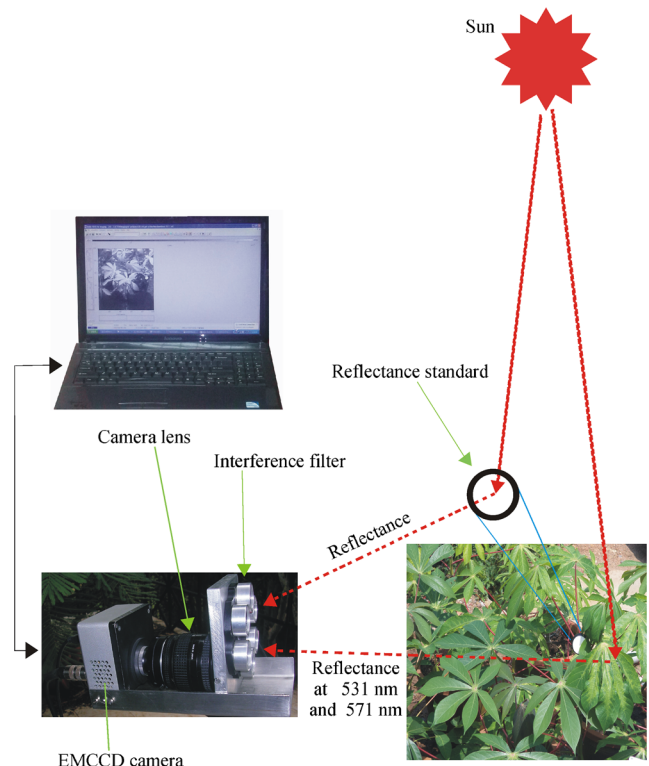


Fig. 2 Multi-spectral reflectance imaging system for proximal imaging of plants

Where, R_λ is the reflectance image of the target at the specified wavelength, I_λ is the raw image of the target at the specified wavelength, r_λ is the raw image of the reflectance standard at the specified wavelength, and K is the reflectance factor of the standard as specified by the manufacturer at each wavelength.

PRI Estimation

Reflectance images of plant leaves were derived by applying Eq. (1) on the captured images at 531 nm and 571 nm. PRI is then estimated using the following relation (Gamon et al. 1997; Penuelas et al. 1995):

$$\text{PRI} = (R_{531} - R_{571}) / (R_{531} + R_{571}) \quad (2)$$

Where, R_{531} and R_{571} denote the solar reflectance of the plant leaves at 531 nm and 571 nm, respectively. In order to correct the shifts, if any, in the x-y coordinates of the images recorded sequentially through different filters, the image data was coded and executed using Matlab (Ver. 7.0) for pixel to pixel matching, before applying Eq. (2).

Plant Physiological Characteristics

The net photosynthetic rate (Pn) was measured from matured leaves of cassava plants selected for study using a Hand-held Photosynthesis device (Model CI-340, CID Inc., USA) under a fixed external PAR (Photosynthetically Active Radiation) of $1500 \mu\text{mol m}^{-2}$. Following photosynthetic measurements, the Chl content of the same set of cassava leaves was analyzed by the method described by Arnon (1949). Chl from the leaf samples was extracted in 8 ml of dimethyl sulphoxide (DMSO) for 1 h at 65 °C (Mandal et al. 2008). The extracted green solution was decanted making the volume to 10 ml with DMSO and its absorbance was measured at 649 and 665 nm on a spectrophotometer (Model: Evolution 201-UV-Visible, Thermofisher Inc., USA). Nine measurements of Pn and Chl were recorded for each grade of infection in each of the 14 varieties of cassava studied and the mean of these measurements was computed. Relative water content (RWC) which is the appropriate measure of plant water stress in terms of the physiological consequence of cellular water deficit was also measured (Barrs and Weatherley 1962). RWC estimates the current water content of the sampled leaf tissue relative to the maximal water content it can hold at full turgidity and was measured using the following formula,

$$\text{RWC}\% = [(FW - DW) / (TW - DW)] \times 100 \quad (3)$$

Where,

FW fresh weight
TW turgid weight
DW dry weight

To assure proper irrigation, soil moisture content was measured using the gravimetric method which involves taking a volume of soil (24 h after watering), weighing it under wet condition, completely drying it out in an oven for about 24 h and then re-weighing the dry sample and calculating soil moisture percentage from the weight loss (Black 1965). The soil moisture content values of all the varieties remained nearly constant between 25 and 30 %, suggesting proper irrigation during the study period.

Data Analysis

The PRI image intensity values were obtained from nine regions of interest (ROI) randomly selected from each leaf with a specific CMD condition and averaged for 20 sets of data per region. Care was taken to avoid areas of veins in the leaves. The mean PRI intensity values were correlated with Pn and total leaf Chl content values. A scatter plot was drawn in Origin (Ver. 7.0) using the discriminant function score of mean PRI values, and the sensitivity and specificity values for classifying different levels of CMD infection were determined. Receiver operating characteristic (ROC) curves were also constructed using the discriminant function scores to assess the potential of PRI imaging data to differentiate visibly no CMD from initial CMD and initial CMD from advanced CMD infected leaves. In a ROC curve, the true positive rate (how many correct positive results) or Sensitivity is plotted in function of the false positive rate (how many incorrect positive results) or 1-Specificity. The area under the ROC curves (AUC) which is a measure of how well a parameter can distinguish between two classification groups and its 95 % CI, including the true value of AUC was computed. All statistical analysis was conducted using SPSS statistical software (SPSS ver. 16.0).

Results and Discussion

PRI Imaging

The monochrome images obtained using Andor SOLIS software were pseudo-color-mapped (PCM) for easy visualization of variation in the reflectance index (PRI) between normal and CMD stressed regions of the leaves (Fig. 3). Irrespective of the variety, the mean PRI shows an increasing trend with CMD infection and was markedly

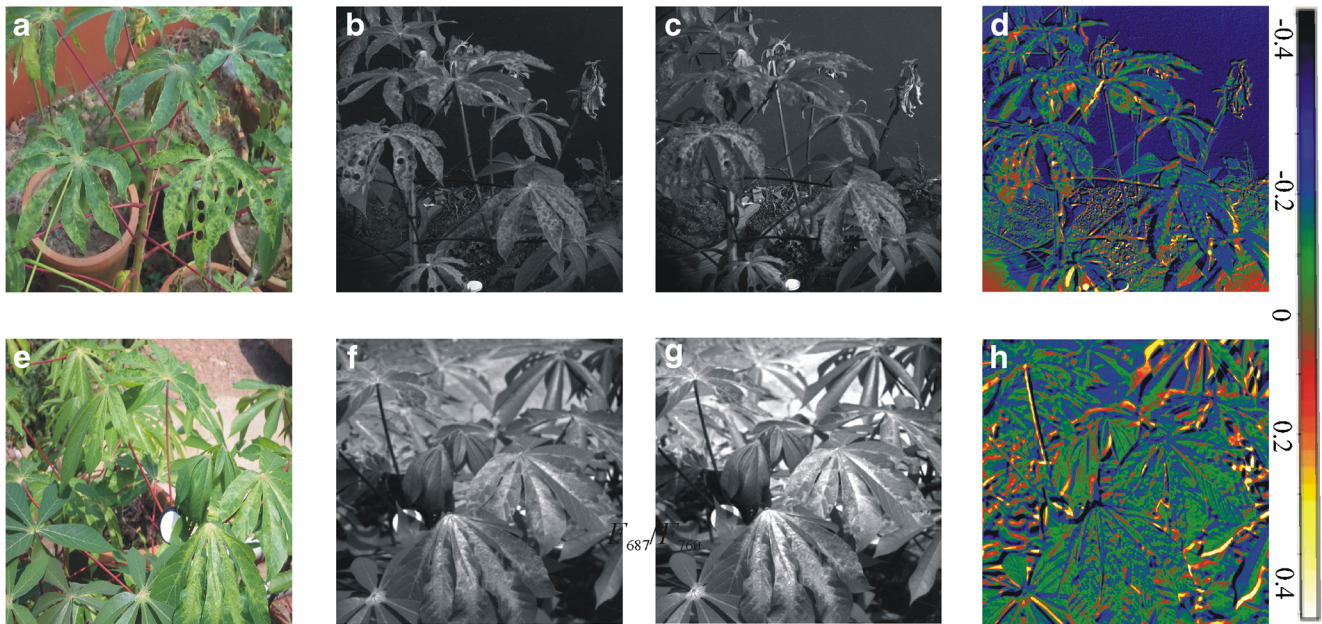


Fig. 3 Photographs of the plant leaf, monochrome reflectance images and pseudo colour mapped (PCM) PRI images of 2 varieties of CMD infected cassava plants. Variety 1 (CI 848): **a** Photo, **b** reflectance image

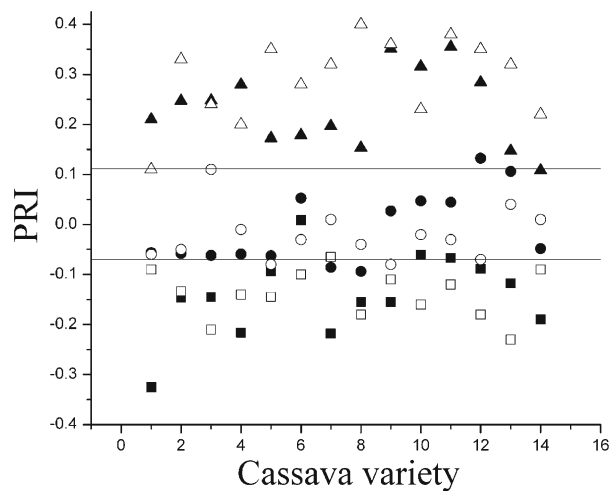
at 531 nm, **c** reflectance image at 571 nm and **d** PRI image. Variety 2 (M-4): **e** Photo, (**f**) reflectance image at 531 nm, **g** reflectance image at 571 nm and **h** PRI image

higher when the level of infection reaches grade-4. The CMD infected regions of the leaves which are visible as yellow spots, are regions with higher PRI values, which indicates inhibition of photosynthetic function. PRI image of the infected regions is represented by light green to yellow colours and it is seen that there is an increase in the PRI values with the progress of stress level. A clear distinction was noticeable in the PRI images between the healthy and chlorosis affected leaves of these plants. Visualization of images of cassava plant (Fig. 3)

provides a clear indication of how CMD infection affects the PRI images. PRI values as low as -0.33 seen in the case of leaves with visibly no symptoms of infection indicate less stressful conditions, whereas the progressively higher values up to 0.46 seen in CMD infected leaves indicate substantial stress. The increase in PRI values with increase in CMD infection shows the effectiveness of the technique in monitoring the level of infection in plants.

PRI images of cassava leaves infected with CMD provide a clear differentiation between different grades of infection,

Fig. 4 Scatter plot diagram based on discriminant function scores for cassava leaves with varying grades of CMD. The solid symbols represent the results of a standard data set ($N = 42$), and open symbols relate to a blind (validation) data set ($N = 42$). The continuous line represents the cut-off value drawn at the mean of data sets belonging to adjoining groups



Standard data set ■ No CMD visible ● Initial CMD ▲ Advanced CMD

Blind data set □ No CMD visible ○ Initial CMD △ Advanced CMD

which is evident from the pseudo coloured PRI images and the PRI values obtained. The colour change from dark blue in less stressed leaves to yellow in CMD stressed leaves could be attributed to changes in plant physiological conditions. Most of the light energy falling on healthy green leaves is utilized for photosynthetic activity, whereas in stressed leaves, to protect the photosynthetic apparatus, the excess energy received is dissipated through various optical processes and as heat, which leads to an increase in reflection at 531 nm.

Scatter Plot Analysis of CMD Infected Cassava Leaves Using PRI Imaging Values

In our study, we have tried to classify different grades of CMD infection in cassava with the help of discrimination scatter plots drawn from the PRI image data. Towards this the five CMD grades (No CMD visible and Grade-1 to Grade-4) were regrouped into three categories, viz. normal/healthy (No CMD visible), Grades 1–2 (initial CMD) and Grades 3–4 (advanced CMD). The discrimination lines were drawn between adjoining groups at the mean of the data values of the two groups-. It was observed that cut off lines discriminating visibly no CMD and initial CMD could be drawn at -0.07, while that between initial CMD and advanced CMD could be drawn at 0.11.

In order to test the reliability of the classification based on PRI image ratio, a blind test was also carried out with 42 readings with known CMD grades. Discriminant function scores of the blind test data were inserted into the training set scatter plot (Fig. 4) for validation. This leads to three out of 14 data in standard set from leaves with visibly no CMD getting misclassified as initial stage (grade-1 or grade-2) of CMD and two each out of 14 data sets of leaves with initial CMD getting misclassified as leaves with no CMD visible and advanced CMD, respectively. However, one data set with advanced CMD (grade-3 or grade-4) infected leaves was misclassified as initial CMD. It was observed that among the blind data set, only one data from visibly no CMD was

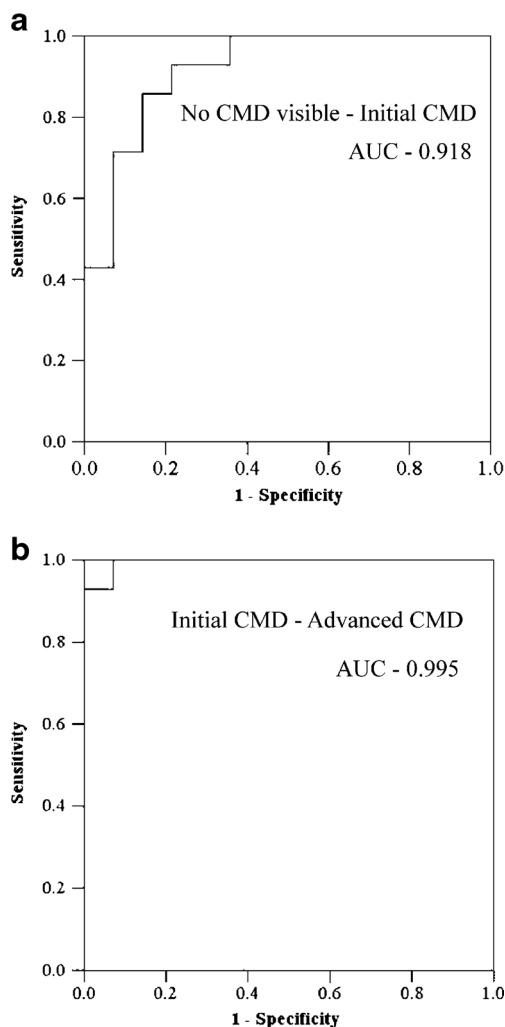


Fig. 5 AUC-ROC shows the discriminatory capacity of PRI image to distinguish between different grades of CMD infection; **a** no visible CMD and initial CMD, and **b** initial CMD and advanced CMD

misclassified as initial CMD, whereas two data from initial CMD was misclassified as no CMD visible and one value was misclassified as advanced CMD. In the advanced CMD group all except one data was misclassified as initial CMD.

Table 2 Overall discrimination accuracy between different grades of cassava mosaic virus disease in cassava leaves obtained using PRI imaging

	Grouping based on CMD infection											
	Visibly no CMD - Initial CMD				Initial CMD - Advanced CMD				Visibly no CMD - Advanced CMD			
	Se (%)	Sp (%)	PPV (%)	NPV (%)	Se (%)	Sp (%)	PPV (%)	NPV (%)	Se (%)	Sp (%)	PPV (%)	NPV (%)
Standard data set	85	79	79	85	93	92	93	92	100	100	100	100
Blind data set	87	92	93	85	92	93	92	93	100	100	100	100
Overall	86	86	86	84	93	93	93	93	100	100	100	100

Sensitivity (Se) true positive/(true positive + false negative), *specificity (Sp)* true negative/(true negative + false positive), *positive predictive value (PPV)* true positive/(true positive + false positive), *negative predictive value (NPV)* true negative/(true negative + false negative)

The above discrimination using standard data resulted in a sensitivity of 85 % and specificity of 79 % for discrimination between leaves with visibly no CMD and initial grades of CMD. The sensitivity and specificity values between initial grades of CMD and advanced grades of CMD was 93 and 92 %, respectively, whereas between leaves with no CMD and those with advanced grade of CMD was 100 %. With blind set of data, the sensitivity and specificity observed for no CMD visible and initial CMD were 87 and 92 % and for initial CMD and advanced CMD were 92 and 93 %, respectively (Table 2).

Discrimination capacity between different grades of CMD infection in cassava leaves was also tested using the receiver operating characteristic (ROC)- curve analysis using SPSS (ver. 16) software. SPSS automatically calculates the sensitivity and specificity of given input ratio values and plots the ROC curves, with sensitivity values against the values of 1-specificity for a default confidence interval of 95 %. AUC-ROC graph showed that initial grade CMD infected leaves can be discriminated from normal leaves with AUC of 0.918, while initial grade CMD infected leaves can be discriminated from advanced grade CMD infected leaves with AUC of

Table 3 Percentage variance of PRI, Pn and Chl for initial and advanced level CMD compared with no visible CMD group in 14 varieties of cassava

Cassava variety	CMD infection level	PRI (%)	Pn (%)	Chl (%)
1	Initial CMD	60	-67	-44
	Advanced CMD	280	-27	-15
2	Initial CMD	59	-70	-46
	Advanced CMD	338	-24	-13
3	Initial CMD	65	-66	-44
	Advanced CMD	167	-57	-32
4	Initial CMD	216	-41	-18
	Advanced CMD	197	-53	-19
5	Initial CMD	41	-74	-37
	Advanced CMD	37	-152	-162
6	Initial CMD	115	-62	-35
	Advanced CMD	167	-42	-51
7	Initial CMD	674	-20	-11
	Advanced CMD	261	-27	-16
8	Initial CMD	73	-64	-32
	Advanced CMD	81	-64	-40
9	Initial CMD	175	-53	-28
	Advanced CMD	230	-37	-18
10	Initial CMD	265	-27	-16
	Advanced CMD	185	-53	-27
11	Initial CMD	72	-63	-36
	Advanced CMD	541	-59	-13
12	Initial CMD	1498	-6	-4
	Advanced CMD	406	-24	-13
13	Initial CMD	158	-23	-33
	Advanced CMD	610	-22	-12
14	Initial CMD	187	-43	-22
	Advanced CMD	237	-29	-17

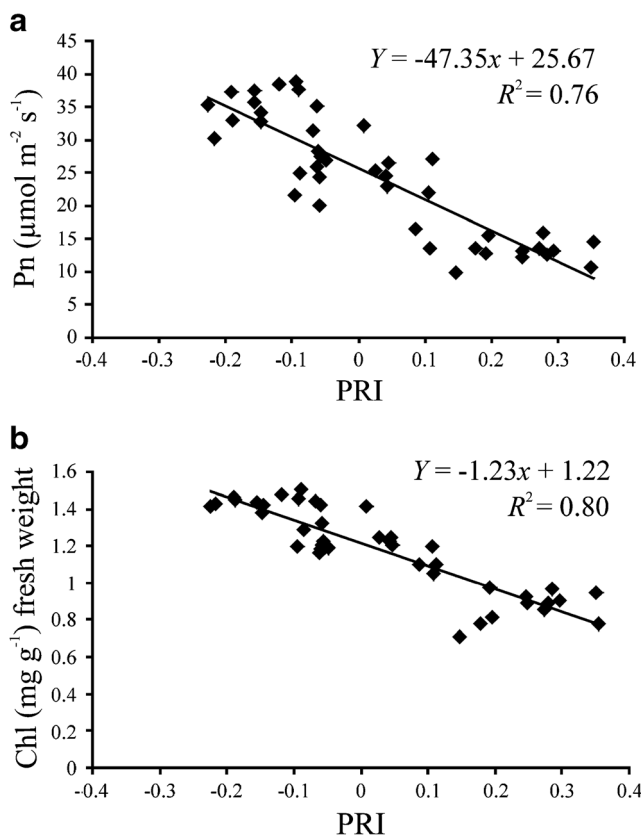


Fig. 6 Correlation of PRI with net photosynthetic rate and total leaf chlorophyll content in 14 varieties of cassava plants with varying degrees of CMD from no visible CMD, initial CMD and advanced CMD ($N = 42$); **a** PRI with net photosynthetic rate, and **b** PRI with total leaf chlorophyll content

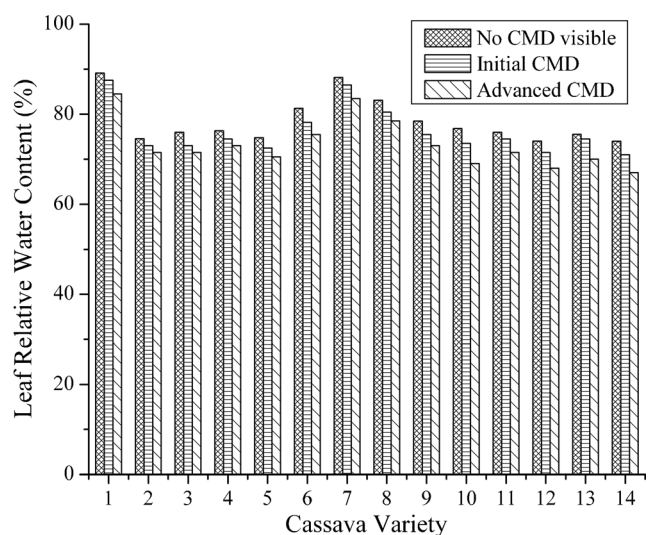


Fig. 7 Variation of leaf Relative Water Content (RWC) in 14 varieties of cassava plants with varying degrees of CMD from no visible CMD, initial CMD and advanced CMD

0.995 (Fig. 5). It is seen that, the AUC for the discrimination score analysis reached nearly 100 % and these results conclusively demonstrate the potential of PRI as a technique to remotely monitor and discriminate the level of CMD infection in cassava plants.

Variance in PRI with Respect to Pn and Total Chl Content

The Pn and total leaf Chl content determined for all the varieties of cassava showed a decreasing trend with the advancement of CMD infection. It is seen that the Pn for leaves without visible CMD symptom varied between 34.02 and 35.55 $\mu\text{mol m}^{-2} \text{s}^{-1}$, whereas, for grade-4 CMD level the value varied between 8.96 and 10.28 $\mu\text{mol m}^{-2} \text{s}^{-1}$ for leaves with advanced CMD infection. Total Chl content of the leaves without visible symptom of CMD lies in the range 1.36–1.51 mg g^{-1} fresh weight and the values decrease to 0.76–0.86 mg g^{-1} fresh weight range in leaves with advanced level of grade-4 CMD infection (Table not shown). Dependence of PRI on Pn and Chl was analyzed for all the varieties of cassava and it was observed that a significant negative linear correlation exists with Pn and Chl (Fig. 6 (a, b)). Taking into consideration the results from all the different varieties of cassava studied, we obtained a correlation coefficient of $R^2 = 0.76$ for PRI with Pn and a correlation coefficient of $R^2 = 0.80$ with Chl content.

The decrease in Pn and total leaf Chl with stress agrees with the reports of previous studies. The reduction in the total leaf Chl content in virus infected leaves could be attributed to the degradation of chloroplasts (Esau 1956), and consequently, reduced and less efficient photosynthetic activity is observed in CMD infected leaves (Tu et al. 1968; Ayanru and Sharma 1982; Palta 1990; Carter 1994; Fang et al. 1998; Raji et al. 2013). The decrease in Pn with stress could be attributed to the closure of the stomata, which reduces the amount of carbon dioxide necessary for photosynthesis (Subhash et al. 2004; Ibaraki et al. 2010). The results suggest the existence of strong inverse relationship between PRI and Pn and between PRI and Chl. On comparing the PRI, Pn and Chl values of different levels of CMD infection with control/no CMD visible group, it is seen that in all cassava plants, irrespective of the variety change, PRI values increased and Pn and Chl values decreased for initial and advanced level of infection (Table 3).

RWC of all the varieties of cassava under study were measured to see how different levels of infection affect the leaf water content (Fig. 7). Towards this grouping of grades 1 and 2 and grades 3 and 4 were done similar to the method followed in scatter plot technique. It is seen that there is a variation in RWC values of the leaves for different grades of CMD infection, which could be attributed to the overall physiological changes occurring during CMD infection.

Conclusions

The main focus of this study was to classify different levels of CMD infection in cassava leaves from the scatter plot of PRI imaging data derived from reflectance images recorded at 531 and 571 nm on a multispectral imaging system developed to record PRI images with sun as the light source. Image processing tools were used to normalize the images for difference in solar irradiance and movement of samples while imaging at different wavelengths. PRI imaging results obtained were comparable to that the changes in Pn and Chl values, and the technique appears to be an effective tool for discrimination of CMD. It was observed that PRI has an inverse linear relationship with Pn and Chl and this makes PRI a useful parameter in the plant stress studies. It is seen from the results that scatter plot diagram of PRI data provides reasonable sensitivity and specificity for classifying different grades of CMD infection. The PRI based technique was evaluated by analyzing blind data sets from randomly selected sites on infected plants. We have obtained a sensitivity of 87 % and specificity of 92 % for discriminating visibly no CMD from initial CMD infection stages. Therefore, it may be concluded that PRI could be utilized as a sensitive tool for classifying CMD infection in cassava plants and to identify early stages of disease when remedial measures could be initiated to stop further damage to the crop.

The results of the study show that proximal sensing technique could be used to mark the difference in degree of CMD infection in plants. This information could be useful during vegetative propagation of new plants, or for extrapolation of the research outcome to other valuable crop species. The accuracies obtained for CMD detection by non-destructive proximal imaging of PRI shows great potential for its application to detect various types of biotic and abiotic stress in plants and provides an opportunity for continuous mapping of plant physiological conditions in forests and farmlands.

Acknowledgments This work was carried out as part of a collaborative project between National Centre for Earth Sciences (NCESS), Thiruvananthapuram and Central Tuber Crop Research Institute (CTCRI), Thiruvananthapuram with grants from the NCESS Plan-289 project. The authors are thankful to the Directors of NCESS and CTCRI, the project assistant (Renju Appukuttan), and the technical staff involved in the work for their encouragement and support. RSN acknowledges NCESS for her research fellowship.

References

- Arnon, D. I. (1949). Copper enzymes in isolated chloroplasts and polyphenol oxidase in *Beta vulgaris*. *Plant Physiology*, 24, 1–15.
- Ayanru, D. K. G., & Sharma, V. C. (1982). Effects of Cassava Mosaic Disease on Certain Leaf Parameters of Field-grown cassava clones. *Phytopathology*, 72, 1057–1059.

- Barrs, H. D., & Weatherley, P. E. (1962). A re-examination of the relative turgidity technique for estimating water deficit in leaves. *Australian Journal of Biological Sciences*, 15, 413–428.
- Bilger, W., & Bjorkman, O. (1990). Role of the xanthophyll cycle in photoprotection elucidated by measurements of light-induced absorbance changes, fluorescence and photosynthesis in leaves of *Hedera canariensis*. *Photosynthesis Research*, 25, 173–185.
- Black, C. A. (1965). Methods of soil analysis: Part I Physical and mineralogical properties. In *American Society of Agronomy*. Madison, Wisconsin: USA.
- Carter, G. A. (1994). Ratios of leaf reflectance in narrow wavebands as indicators of plant stress. *International Journal of Remote Sensing*, 15, 697–703.
- Carter, G. A., & Miller, R. L. (1994). Early Detection of Plant Stress by Digital Imaging within Narrow Stress-Sensitive Wavebands. *Remote Sensing of Environment*, 50, 295–302.
- Deery, D., Jimenez-Berni, J., Jones, H., Sirault, X., & Furbank, R. (2014). Proximal remote sensing buggies and potential applications for field based phenotyping. *Agronomy*, 5, 349–379.
- Demmig-Adams, B., & Adams, B. (1994). The role of xanthophyll cycle carotenoids in the protection of photosynthesis. *Trends in Plant Science*, 1, 21–26.
- Esau, K. (1956). An anatomical view of virus disease. *American Journal of Botany*, 43, 739–748.
- Fang, Z., Bouwkamp, J., & Solomos, T. (1998). Chlorophyllase activities and chlorophyll degradation during leaf senescence in non-yellowing mutant and wild type of *Phaseolus vulgaris* L. *Journal of Experimental Botany*, 49, 503–510.
- Filella, I., Porcar-Castell, A., Munne-Bosch, S., Back, J., Garbulsky, M. F., & Penuelas, J. (2009). PRI assessment of long-term changes in carotenoids/chlorophyll ratio and short-term changes in de-epoxidation state of the xanthophyll cycle. *International Journal of Remote Sensing*, 30, 4443–4455.
- Gamon, J. A., Peñuelas, J., & Field, C. B. (1992). A narrow-wave band spectral index that track diurnal changes in photosynthetic efficiency. *Remote Sensing of Environment*, 41, 35–44.
- Gamon, J. A., Serrano, L., & Surfus, J. S. (1997). The Photochemical Reflectance Index: An optical indicator of photosynthetic radiation use efficiency across species, functional types and nutrient levels. *Oecologia*, 112, 492–501.
- Ibaraki, Y., Matsumura, K., & Gupta, S. D. (2010). Low Cost Photochemical reflectance index measurements of micro propagated plantlets using image analysis. *Computers and Electronics in Agriculture*, 71, 170–175.
- Mandal, M., Saravanan, R., & Maiti, S. (2008). Effect of different levels of N, P and K on downy mildew (*Peronospora plantaginis*) and seed yield of isabgol (*Plantago ovate*). *Crop Protection*, 27, 988–955.
- Nakaji, T., Oguma, H., & Fujinuma, Y. (2006). Seasonal changes in the relationship between photochemical reflectance index and photosynthetic light use efficiency of Japanese larch needles. *International Journal of Remote Sensing*, 27, 493–509.
- Nichol, C. J., & Grace, J. (2010). Determination of leaf pigment content in *Calluna vulgaris* shoots from spectral reflectance. *International Journal of Remote Sensing*, 31, 5409–5422.
- Palta, J. (1990). Leaf chlorophyll content. Instrumentation for studying vegetation canopies for Remote Sensing in Optical and Thermal Infrared Regions. *Remote Sensing Reviews*, 5(1), 207–213.
- Panigada, C., Rossini, M., Meroni, M., Cilia, C., Busetto, L., Amaducci, S., Boschetti, M., Cogliati, S., Picchi, V., Pinto, F., Marchesi, A., & Colombo, R. (2014). Fluorescence, PRI and canopy temperature for water stress detection in cereal crops. *International Journal of Applied Earth Observation and Geoinformation*, 30, 167–178.
- Patil, B. L., & Fauquet, C. M. (2009). Cassava mosaic geminiviruses: actual knowledge and perspectives. *Molecular Plant Pathology*, 10(5), 685–701.
- Penuelas, J., Gamon, J. A., Fredeen, A. L., Merino, J., & Field, C. B. (1994). Reflectance indices associated with physiological changes in nitrogen- and water-limited sunflower leaves. *Remote Sensing of Environment*, 48, 135–146.
- Penuelas, J., Filella, I., & Gamon, J. A. (1995). Assessment of photosynthetic radiation use efficiency with spectral reflectance. *New Phytologist*, 131, 291–296.
- Penuelas, J., Llusia, J., Pinol, J., & Filella, I. (1997). Photochemical reflectance index and leaf photosynthetic radiation use efficiency assessment in Mediterranean trees. *International Journal of Remote Sensing*, 18, 2863–2868.
- Raji, S. N., Ravi, V., Saravanan, R., Subhash, N., Makesh Kumar, T., Nita, S., & Renju, U. A. (2013). Assessing cassava mosaic virus infection in cassava plants using PRI imaging. Proceedings of *National Symposium on Pathogenomics for Diagnosis and Management of Plant Diseases*, Thiruvananthapuram, India, October 25–26.
- Raji, S. N., Subhash, N., Ravi, V., Saravanan, R., Mohanan, C. N., Nita, S., & Makesh Kumar, T. (2015). Detection of mosaic virus disease in cassava plants by sunlight-induced fluorescence imaging: a pilot study for proximal sensing. *International Journal of Remote Sensing*, 36(11), 2880–2897.
- Richardson, A. D., & Berlyn, G. P. (2002). Spectral reflectance and photosynthetic properties of *Betula papyrifera* (Betulaceae) leaves along an elevational gradient on Mt. Mansfield, Vermont, USA. *American Journal of Botany*, 89, 88–94.
- Richardson, A. D., Berlyn, G. P., & Duigan, S. P. (2003). Reflectance of Alaskan black spruce foliage in relation to elevation and latitude. *Tree Physiology*, 23, 537–544.
- Subhash, N., Mohanan, C. N., Rupananda, J. M., & Muralidharan, V. (2004). Quantification of stress adaptation by laser-induced fluorescence spectroscopy of plants exposed to engine exhaust emission and drought. *Functional Plant Biology*, 31, 709–719.
- Terry, E.R. (1975). Description and evaluation of cassava mosaic disease in Africa. Proceedings of Interdisciplinary workshop held at IITA, Ibadan, Nigeria, 75, 53–54.
- Thresh, J. M., Fargette, D., & Otim Nape, G. W. (1994). Effects of African cassava mosaic geminivirus on the yield of cassava. *Tropical Science*, 34, 26–42.
- Tu, J. C., Ford, R. E., & Krass, C. J. (1968). Comparison of chloroplasts and photosynthetic rates of plants infected and not infected by maize dwarf mosaic virus. *Phytopathology*, 58, 285–288.
- Whitehead, D., Boelman, N. T., Turnbull, M. H., Griffin, K. L., Tissue, D. T., Barbour, M. M., Hunt, J. E., Richardson, S. J., & Peltzer, D. A. (2005). Photosynthesis and reflectance indices for rainforest species in ecosystems undergoing progression along a soil fertility chronosequence in New Zealand. *Oecologia*, 144, 233–244.